PHYSICAL REVIEW B VOLUME 62, NUMBER 10 1 SEPTEMBER 2000-II

Evidence for spiral magnetic order in the heavy fermion material $CeRhIn_5$

N. J. Curro,[1] P. C. Hammel,[1] P. G. Pagliuso,[1] J. L. Sarrao,[1] J. D. Thompson,[1] and Z. Fisk[2]
[1]*Condensed Matter and Thermal Physics, Los Alamos National Laboratory, Los Alamos, New Mexico 87545*
[2]*National High Magnetic Field Laboratory and Florida State University, Tallahassee, Florida 32306*
(Received 6 June 2000)

We report ^{115}In nuclear quadrupolar resonance measurements of the heavy fermion compound $CeRhIn_5$ in the paramagnetic and antiferromagnetic states. The magnetic order is consistent with a model of helical modulation of the Ce moments that is incommensurate with the lattice, and the magnetic dynamics indicate possible two-dimensional behavior.

The interplay between magnetism and superconductivity in heavy fermion materials has attracted much interest since the discovery of heavy fermion superconductivity.[1] In several of the Ce based heavy fermion compounds, the behavior of the magnetic order can be understood qualitatively in terms of a simple picture, in which long-range Ruderman-Kittel-Kasuya-Yosida (RKKY) interactions between the Ce moments compete with short-range Kondo interactions.[2] In this picture, both the RKKY and the Kondo interactions depend on a coupling constant J that can be tuned with pressure or chemical substitution. Since each of these interactions evolves differently with J, the nature of the ground state can change drastically with pressure or chemical substitution. Recent experimental work indicates that when the many-body Kondo effect dominates (large J), the system undergoes a zero-temperature magnetic-nonmagnetic transition. In $CeIn_3$ and $CePd_2Si_2$, both of which have antiferromagnetic ground states at ambient pressure, T_N decreases monotonically with pressure and superconductivity develops close to the magnetic instability where T_N vanishes.[3] Transport measurements indicate that these systems exhibit unusual non-Fermi-liquid behavior near this point, supporting the idea that the physics of these materials is dominated by proximity to a quantum critical point, and it has been suggested that the superconductivity in these materials is mediated by spin fluctuations near this boundary.[3]

Recently a very interesting class of heavy fermion materials with the formula $Ce_mM_nIn_{3m+2n}$, where M is Rh or Ir, was studied.[4] $CeRhIn_5$ is an antiferromagnet at ambient pressure with $T_N=3.8$ K, and becomes a superconductor with $T_c=2.1$ K above a critical pressure $P_c\sim 16$ kbar. $CeRhIn_5$ differs somewhat from other Ce based heavy fermion materials in that the magnetic-nonmagnetic transition where superconductivity develops is apparently a first-order transition.[4] It has been suggested that $CeRhIn_5$ exhibits two-dimensional (2D) magnetic character, thus the magnetic behavior and the origin of the superconductivity may be related to that of the cuprates. A detailed understanding of the magnetism is crucial in order to understand how the antiferromagnetism evolves into superconductivity.

Here we report ^{115}In nuclear quadrupolar resonance (NQR) ($I=9/2$) measurements at ambient pressure in a powder sample of $CeRhIn_5$ in the paramagnetic and antiferromagnetic states. NQR is an ideal probe of the local magnetic fields in the unit cell as well as the dynamic behavior of the electronic system. In the paramagnetic state we find metallic behavior. Just above T_N, the magnetic correlations slow down, dominating the spin-lattice relaxation. Below T_N we observe the rapid development of an internal field that indicates that the magnetism is localized on Ce sites with a moment $\mu_{Ce}\sim 0.1-0.2\mu_B$. The NQR spectrum in the antiferromagnetic state indicates a spiral modulation of the Ce moments that is incommensurate with the lattice.

Crystals of $CeRhIn_5$ grown from an In flux were ground to a powder in order to facilitate the penetration of the rf fields necessary for NQR. Roughly speaking, $CeRhIn_5$ consists of alternating layers of $CeIn_3$ and $RhIn_2$ and so has two inequivalent In sites per unit cell. The In(1) site, analogous to the single In site in cubic $CeIn_3$, is located on the top and bottom faces of the tetragonal unit cell. There are four In(2) sites per unit cell, two on each of the lateral faces of the unit cell, equidistant above and below the Rh layer. The NQR spectrum in the paramagnetic state at 4 K reveals two sets of resonances associated with the two In sites: site A is characterized by $\nu_Q=6.78\pm 0.01$ MHz and $\eta=0.0$, whereas site B is characterized by $\nu_Q=16.665\pm 0.001$ MHz and $\eta=0.445\pm 0.001$, where ν_Q and η are defined by the NQR Hamiltonian: $\mathcal{H}_Q=(h\nu_Q/6)[3I_z^2-I^2+\eta(I_x^2-I_y^2)]$. Here I is the nuclear spin, $\nu_Q\equiv eQV_{zz}/6I(2I+1)$, Q is the quadrupolar moment of the nucleus, $V_{\alpha\alpha}$ is the electric field gradient along the α direction, and $\eta\equiv(V_{xx}-V_{yy})/V_{zz}$ following the convention $V_{zz}>V_{xx}>V_{yy}$.[5] In zero field, there are four transitions per site; experimentally these are quite narrow [full width at half maximum (FWHM) $\sim$75 kHz] indicating a small distribution of electric field gradients and thus a high-quality sample. By considering the symmetry of the two In sites in the crystal, we assign the axially symmetric A site to In(1) and the lower symmetry site B to In(2); this assignment is further supported by the intensity ratio. A simple point-charge calculation indicates that the electric-field-gradient (EFG) vector $\mathbf{q}$ (the principal axis of the EFG tensor with the largest eigenvalue) points along the crystal c axis for In(1) and points inward towards the center of the unit cell (along the crystal a or b axes) for In(2). Therefore for In(1) the z axis lies along the crystal c direction, and for In(2) the z axis lies along crystal a or b directions. Furthermore, for the In(2) the x axis lies along the crystal c direction.

In order to measure the internal field in the antiferromagnetic state, we consider the splitting of the In(1) spectrum by

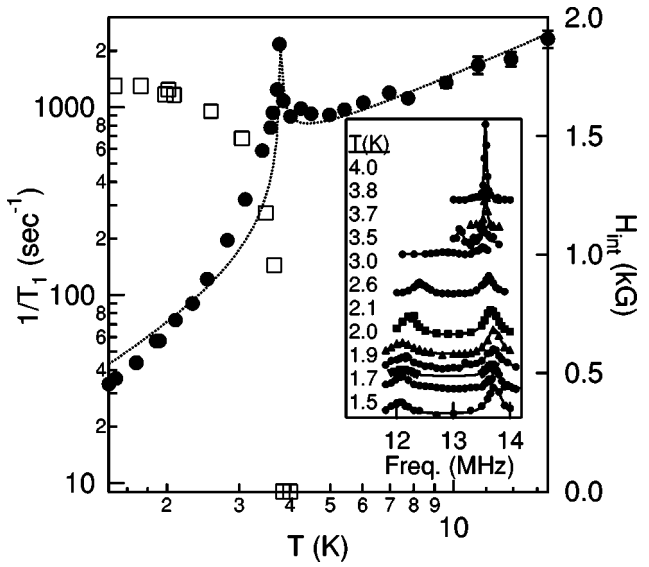

FIG. 1. The internal field (□) and the spin-lattice relaxation rate (●) at the In(1) site. The dotted line is a fit to the SCR theory of antiferromagnetic fluctuations (see text). Inset: The temperature dependence of the $2\nu_Q$ transition.

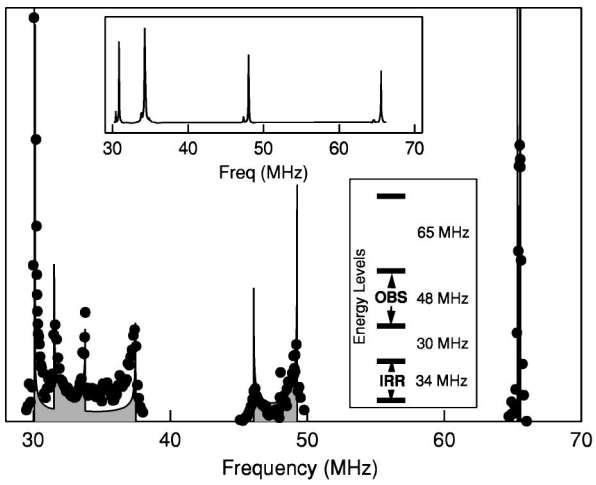

FIG. 2. The spectrum of the In(2) site at 1.5 K in the Néel state. The filled region is a fit as described in the text. Inset: The In(2) spectrum in the paramagnetic state at 4 K. The small peaks to the left of the main peaks are signals from the low abundance ^{113}In isotope. A schematic In(2) nuclear-spin energy-level diagram indicating the transitions used in the SEDOR experiment is shown.

an internal field. In the absence of such a field, the In(1) spectrum consists of four transitions given by $\nu = n\nu_Q$, where $n = 1,2,3$, or 4. The $2\nu_Q$ $(3/2 \leftrightarrow 5/2)$ transition is shown as a function of temperature in the inset to Fig. 1. In the presence of a nonzero internal field the nuclear Hamiltonian must include the Zeeman term $\mathcal{H}_Z = \gamma\hbar \mathbf{I}\cdot\mathbf{H}_{\rm int}$. Here γ is the gyromagnetic ratio and $\mathbf{H}_{\rm int}$ is the internal field at the In site. For $\gamma H_{\rm int} < \nu_Q$, the NQR resonance lines are split by the internal field. We find that the $3\nu_Q$ and $4\nu_Q$ transitions are unaffected by $H_{\rm int}$, but the $2\nu_Q$ transition is split into two resonances that are asymmetric with respect to the original transition (Fig. 1 inset). If there were a component of the internal field along the c axis then all of the transitions would be split equally by γH_c; there is no such splitting. Thus $\mathbf{H}_{\rm int}$ lies in the ab plane.

We diagonalize the full Hamiltonian $\mathcal{H}_{\rm nuc} = \mathcal{H}_Q + \mathcal{H}_Z$ and determine $\mathbf{H}_{\rm int}$ as a function of temperature from the resonance positions shown in the inset to Fig. 1; the results are shown in Fig. 1. The internal field of 1.7 kG at the In(1) site can be compared with an internal field of 5.0 kG at the equivalent In site in $CeIn_3$,[6] where neutron-scattering measurements indicate a Ce moment of $0.4\mu_B$.[7] Assuming a similar hyperfine coupling, the Ce moment in $CeRhIn_5$ is ~ 0.1–$0.2\mu_B$. The direction of the Ce moments within the ab plane cannot be determined because the field gradient at the In(1) site is axially symmetric about the c axis, thus the splitting of the NQR transition is sensitive only to the magnitude of the internal field. Note, however, that the sharp lines in the antiferromagnetic state (see the inset of Fig. 1) indicate that there exists a single value of the magnitude of the internal field.

The growth of the sublattice magnetization below T_N is quite rapid: a fit to $H_{\rm int}$ versus $(1 - T/T_N)^\beta$ gives $\beta = 0.25 \pm 0.03$, much faster than mean field ($\beta = 0.5$). It is interesting to compare this result with a similar result found in the cuprate antiferromagnet La_2CuO_4, in which the transition to the antiferromagnetic state is almost first-order-like, with critical exponent $\beta \sim 0.1$.[8] Note that the reduced critical exponent in La_2CuO_4 is related to the two-dimensional magnetism in this material; the reduced exponent in $CeRhIn_5$ may also indicate 2D magnetic behavior.

The spin lattice relaxation rate (T_1^{-1}) of the In(1) (Fig. 1) was measured as a function of T by fitting the recovery of the magnetization at the $4\nu_Q$ transition to equilibrium after an inversion pulse. This transition exhibits no splitting due to the internal field in the antiferromagnet state. The time dependence of the recovery was well fit to the expected multiexponential recovery for a spin 9/2 nucleus[9] using a single T_1 at all temperatures. T_1^{-1} exhibits critical fluctuations within ~ 1–2 K of T_N; this behavior contrasts with that of $CeIn_3$, which shows no critical slowing down through $T_N (= 10\ {\rm K})$.[6] The dotted line through the data in Fig. 1 is a fit to the Moriya *et al.* theory for self-consistent renormalized (SCR) spin fluctuations for weak itinerant antiferromagnets:[10]

$$\frac{1}{T_1} = \begin{cases} aT + bT/\sqrt{T - T_N} & \text{for } T > T_N \\ cT/M(T) & \text{for } T < T_N, \end{cases}$$

where $a = 133\ ({\rm s\,K})^{-1}$, $b = 41.1\ {\rm s}^{-1}\ {\rm K}^{-1/2}$, and $c/M_0 = 12.5\ ({\rm s\,K})^{-1}$ are fitting parameters, and $M(T) = M_0(1 - T/T_N)^{0.25}$ is the antiferromagnetic order parameter. The SCR expression for T_1^{-1} has been used successfully to fit the $T_1^{-1}(T)$ in other heavy fermion materials which exhibit magnetic order,[11] however, it fails to capture all of the behavior below T_N in $CeRhIn_5$, perhaps reflecting enhanced fluctuations associated with the 2D character. The first term in the expression allows for a Korringa-type relaxation expected in a metal. Above 10 K $CeRhIn_5$ is metallic, and $\rho \leqslant 10\,\mu\Omega$ cm. Below T_N, spin-lattice relaxation due to quasiparticles at the Fermi surface is suppressed as magnetism develops.

Figure 2 shows the NQR spectrum of the In(2) site in the paramagnetic and antiferromagnetic states. Since this site is not axially symmetric, the transition frequencies do not pos-

sess a simple relationship as do those of the In(1) site. In the paramagnetic state the spectrum consists of four sharp transitions; however, as the internal field develops below T_N the low-frequency lines broaden (by several MHz) and exhibit a pattern which indicates a distribution of internal fields. The electric field gradient at the In(1) site is axially symmetric; in contrast, the spectrum of the In(2) site is sensitive not only to the azimuthal angle between $\mathbf{H}_{\rm int}$ and the EFG (along a or b for this site), but to the polar angle as well. The fact that the transitions at 48 and 65 MHz are affected less than the low frequency transition demonstrates that $H_{\rm int}$ has no component parallel to the EFG, for if it did then each transition would experience an equal splitting $\gamma H_{\rm int}$. We find good agreement between the measured spectrum and a simulation assuming the internal field varies along the c axis as $H_{\rm int} = H_0 \cos(2\pi z/\lambda)$. We numerically diagonalize the summed quadrupolar and Zeeman Hamiltonian to obtain the transition frequencies; these are then weighted by the probability of a given internal field $H_{\rm int}$ to generate the simulated spectrum shown in Fig. 2 (shaded regions). Using a maximum field $H_0 = 2.7$ kG, all of the relevant features in the spectrum are accurately reproduced; this strongly indicates the broadening results from a distribution of internal fields.

The continuous nature of the broadened In(2) spectrum implies a spatially modulated magnetic structure incommensurate with the lattice (or having a very long period). The In(1) spectrum, however, implies a single magnitude of the internal field; a distribution of magnitudes would cause the In(1) spectrum to also broaden into a powder patternlike distribution. Therefore we are led to consider a spiral modulation where the orientation of the Ce moment rotates in the ab plane. Without a detailed knowledge of the transferred hyperfine couplings one cannot completely determine $H_{\rm int}$ at each site, however, we estimate $H_{\rm int}$ for this type of structure by calculating the direct dipolar field at both the In(1) and In(2) sites. We assume that the magnetic moments are localized on Ce sites, and the spiral twists along the c axis: $\boldsymbol{\mu}_{nml} = \mu_{\rm Ce}(-1)^{n+m+l}[\mathbf{a}\cos(klc) + \mathbf{b}\sin(klc)]$, where $\boldsymbol{\mu}_{nml}$ is the moment on the Ce located at $\mathbf{r} = n\mathbf{a} + m\mathbf{b} + l\mathbf{c}$, and $k = 2\pi/\lambda$, where λ is the wavelength of the modulation. This structure gives rise to an internal field at the In(1) site which lies in the ab plane, remains constant in magnitude, but varies in angle in the ab plane. This result is entirely consistent with the spectrum of the In(1). This magnetic structure distinguishes half of the In(2) sites from the others: two of the four sites experience a field $H_{2a} = \pm H_0 \cos(2\pi lc/\lambda)$ along the c axis and the other two sites experience a field $H_{2b} = \pm H_0 \sin(2\pi lc/\lambda)$, also along the c axis. Hence both types of In(2) sites experience the same *distribution* of internal fields. For In(2) the summed contributions from all Ce moments result in a net internal field along the c axis with no components in the ab plane.

Further insight into the magnetic structure can be obtained by performing spin echo double resonance (SEDOR) between nearest-neighbor In(2) nuclei along the c axis.[5] Since only neighboring nuclei are correlated (via a short-range magnetic interaction), SEDOR can determine the difference in resonance frequencies between neighboring unlike nuclei. In the antiferromagnetic state of $CeRhIn_5$ neighboring In(2) nuclei along the spiral direction experience different internal fields, rendering them unlike. By applying SEDOR inversion pulses at a set frequency and searching the spectrum for a SEDOR reduction at a different observe frequency, one can determine the frequency difference between neighbors and hence deduce the difference in internal field and the pitch of the spiral. One important aspect of such a scheme is that normally SEDOR is performed between two different nuclear species which resonate at different frequencies, whereas in this case we conduct SEDOR between nuclei of the same species. One can perform SEDOR between two like nuclei if they possess multiple nuclear transitions at different frequencies. However, if the two transitions are neighboring transitions, the SEDOR pulse will create a higher-order coherence, which is undesired.[5]

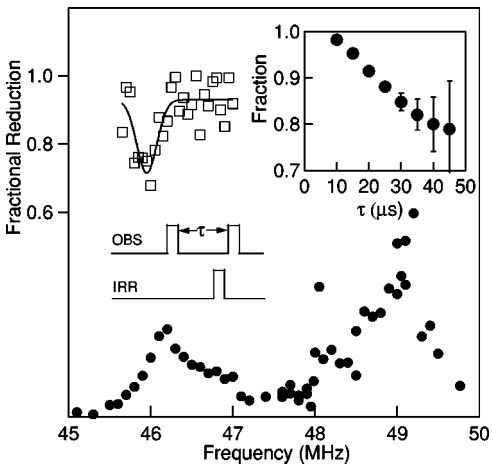

FIG. 3. The SEDOR reduction across the spectrum in the antiferromagnetic state: single resonance spectrum (●); the SEDOR reduction as a function of frequency (□), where the SEDOR pulse is applied at 37.2 MHz (see Fig. 2), and $\tau = 70$ μsec. The solid line is a Gaussian fit to the data with center frequency 45.95 MHz and FWHM 0.31 MHz. Inset: The SEDOR reduction as a function of τ in the paramagnetic state at 4 K. Spin echoes were acquired at 48 MHz while SEDOR pulses were applied at 34.2 MHz. Plotted is the echo integral obtained with the SEDOR pulse normalized to the echo integral obtained without.

To demonstrate the viability of such an experiment we measured the SEDOR reduction between different nuclear transitions of the In(2) in the paramagnetic state. We employed the double-resonance probe design of Haase *et al.*, which allows one to tune to close frequencies.[12] The inset of Fig. 3 shows the SEDOR reduction as a function of the pulse spacing. Here the 48 MHz transition is observed with a standard echo sequence, and a π pulse is applied to the 34 MHz transition (see inset, Fig. 2). The echo reduction with increasing pulse spacing clearly indicates a strong coupling between In(2) neighbors.

Figure 3 presents the SEDOR data in the antiferromagnetic state. Here the SEDOR irradiation (IRR) pulse is applied slightly below the 37 MHz horn (see Fig. 2), and the observed frequency is swept from 45 to 50 MHz. The irradiation frequency corresponds to an internal field $H_0 = 2.29$ kG; if the coupled nucleus experienced the same internal field one would expect a correlation at 46.3 MHz at the higher nuclear transition. Instead, there is a clear decrease in the echo integral at 45.95 MHz corresponding to an internal field of 2.63 ± 0.31 kG (obtained by diagonalization of $\mathcal{H}_{\rm nuc}$). This increased internal field experienced by the nearest In(2)

neighbor of the irradiated nucleus (separated along the c axis by a distance $0.38c$ where $c=6.782$ Å is the lattice spacing[13]) implies a wavelength $\lambda=4.6c\pm0.8c$ assuming that the internal field varies as $\cos(2\pi z/\lambda)$. Note that there is a component of the SEDOR fraction that is independent of frequency, i.e., the signal is reduced by approximately 10%. The origin of this offset is not understood, but may be related to higher-order coherences generated by the SEDOR π pulse on the observed nuclei. We are currently investigating this effect in greater depth.

A well-known class of helical antiferromagnets includes the rare-earth metals Ho, Dy, and Tb, where the magnetic coupling is given by the RKKY interaction. A model Hamiltonian that can give rise to the magnetic structure seen in these materials as well as in $CeRhIn_5$ is one in which the couplings between all nearest-neighbor pairs, J_1, is antiferromagnetic and along one particular direction the couplings between next-nearest-neighbor pairs, J_2, is ferromagnetic.[14] The frustration between the two competing interactions gives rise to the spiral along the c direction when $|J_2/J_1|$ exceeds a critical value. It is not unreasonable to expect that such interactions may be present in $CeRhIn_5$.

Spiral magnetic order along the c axis can also explain the unusual anisotropy of the bulk magnetic susceptibility $\chi(T)$. In the paramagnetic state $\chi^{-1}\propto T$ for $T>100$ K, with Curie-Weiss constant $\theta_c=-79$ K for H along the c axis, and $\theta_{ab}=+16$ K for H in the ab plane.[4] Although anisotropic crystal-field effects cannot be excluded, such a result could arise if the average coupling along the c direction were ferromagnetic, and the average coupling in the plane were antiferromagnetic. Furthermore, $\chi_c(T)\sim2\chi_{ab}(T)$, suggesting that the easy axis is along the spiral direction. This picture is further supported by de Haas–van Alphen and magnetization measurements, which reveal a magnetic transition in fields on the order of 2 T along the c axis.[15] The behavior of this transition is consistent with an anisotropic antiferromagnetic spin-density wave or helical magnetic order. Finally, recent elastic neutron-scattering results indicate an incommensurate spin modulation along the c direction with period $3.3c$.[16]

We thank N. Hasselmann, A. Suter, and C. P. Slichter for inspiring discussions, and especially C. P. Slichter for suggesting the SEDOR experiment. This work was performed under the auspices of the U.S. Department of Energy.

[1] F. Steglich *et al.*, Phys. Rev. Lett. **43**, 1892 (1979).
[2] S. Doniach, in *Valence Instabilities and Related Band Phenomenoa*, edited by R. D. Parks (Plenum, New York, 1977), p. 169.
[3] N. D. Mathur *et al.*, Nature (London) **394**, 39 (1998).
[4] H. Hegger *et al.*, Phys. Rev. Lett. **84**, 4986 (2000).
[5] C. P. Slichter, *Principles of Magnetic Resonance*, 3rd. ed. (Springer-Verlag, New York, 1990).
[6] Y. Kohori *et al.*, Physica B **259-261**, 103 (1999).
[7] J. M. Lawrence *et al.*, Phys. Rev. B **22**, 4379 (1980).
[8] D. E. MacLaughlin *et al.*, Phys. Rev. Lett. **72**, 760 (1994).
[9] A. Narath, Phys. Rev. **162**, 320 (1967).
[10] T. Moriya *et al.*, Solid State Commun. **15**, 169 (1974).
[11] M. Kyogaku *et al.*, J. Phys. Soc. Jpn. **62**, 4016 (1993).
[12] J. Haase *et al.*, J. Magn. Reson. **135**, 273 (1998).
[13] J. L. Sarrao (private communication).
[14] H. Kawamura, J. Phys.: Condens. Matter **10**, 4707 (1998).
[15] A. L. Cornelius *et al.* (unpublished).
[16] W. Bao (private communication).